

# Synthesis and Characterization of PNIPAM/PS Core/Shell Particles

Li Zhang,<sup>1,2</sup> Eric S. Daniels,<sup>1,3</sup> Victoria L. Dimonie,<sup>1</sup> Andrew Klein<sup>1,3</sup>

<sup>1</sup>*Emulsion Polymers Institute, Lehigh University, Bethlehem, Pennsylvania 18015*

<sup>2</sup>*Department of Chemistry, Lehigh University, Bethlehem, Pennsylvania 18015*

<sup>3</sup>*Department of Chemical Engineering, Lehigh University, Bethlehem, Pennsylvania 18015*

Received 4 February 2009; accepted 27 September 2009

DOI 10.1002/app.31508

Published online 29 June 2010 in Wiley InterScience (www.interscience.wiley.com).

**ABSTRACT:** Crosslinked, monodisperse PNIPAM particles were synthesized by precipitation polymerization. The particle size was measured by dynamic light scattering (DLS), capillary hydrodynamic fractionation (CHDF), and transmission electron microscopy (TEM). Two different polymerization methods were used to prepare PNIPAM/PS core/shell particles, both above and below the volume phase transition temperature (VPPT) using either a semibatch or seeded semibatch polymerization process.

In both processes, uniform “raspberry” structures were obtained in which polystyrene formed small domains on the surface of the PNIPAM particles. The resulting core and shell structure was confirmed by temperature-dependent particle size and density gradient experiments. © 2010 Wiley Periodicals, Inc. *J Appl Polym Sci* 118: 2502–2511, 2010

**Key words:** core-shell polymers; latexes; precipitation polymerization; stimuli-sensitive polymers; gels; colloids

## INTRODUCTION

In recent years, a great deal of interest has been focused on thermosensitive polymers which exhibit a fast reversible change from a hydrophilic to a hydrophobic structure. This change occurs at a temperature, termed the lower critical solution temperature (LCST), below which all compositions are miscible and above which phase separation occurs. This transition temperature is also called the volume phase transition temperature (VPTT) specifically for thermosensitive polymer microspheres due to their large volume change during the transition. Among all of the thermosensitive polymers, poly(*N*-isopropylacrylamide) (PNIPAM) is the most well known and profoundly studied one with a LCST  $\sim$  31–32°C.

Polystyrene-based colloidal polymer particles have been widely utilized as carriers for bio-diagnostic applications.<sup>1</sup> The unique properties of PNIPAM inspired researchers to combine PNIPAM with polystyrene (PS) in areas such as biomedical<sup>2</sup> and bio-separations,<sup>3</sup> drug delivery,<sup>4</sup> catalysts,<sup>5</sup> and pollution control.<sup>6</sup> However, it is interesting to note that almost all of the research reported in the literature focused on synthesizing a PNIPAM shell around a PS core (or similar other polymeric materials),<sup>7–10</sup> although there are several studies describing the

synthesis of a PNIPAM-based core and a PS shell.<sup>11,12</sup> It is thermodynamically favorable to form a hydrophilic shell around a hydrophobic core. The PNIPAM/PS core and shell structure is not only thermodynamically challenging to synthesize, but also represents a unique morphology. The core can undergo a temperature-dependent phase change, from a gel to polymer with free water.<sup>13–15</sup>

Pelton was the first to study the copolymerization of NIPAM and styrene as well as grafting PNIPAM on prepared polystyrene and polystyrene-butadiene latex surfaces by emulsifier-free and crosslinker-free methods.<sup>16</sup> The obtained particles exhibited temperature-dependent colloidal stability. Subsequently, several other researchers reported the preparation of PNIPAM<sup>17,18</sup> or poly(styrene-*N*-isopropylacrylamide) microspheres.<sup>19–21</sup> Generally, a two-stage procedure was utilized to prepare this type of particle. First, a mixture of styrene and NIPAM monomers were copolymerized by an emulsifier-free batch polymerization method. In a second stage, a PNIPAM shell layer was then fabricated onto the core seeds prepared in the first stage. In another report, another research group described the encapsulation of PNIPAM with PS to form hollow particles using a two-stage polymerization process.<sup>12</sup> Cationic copolymer was utilized to form PNIPAM microspheres in the first stage of this process. Styrene and crosslinker were added during the shell formation step.

In this research, particles were prepared with PNIPAM as a core and PS as a shell. As each PNIPAM particle can contain as much as  $\sim$  95 wt % water,

Correspondence to: A. Klein (ak04@lehigh.edu).

TABLE I  
NIPAM Emulsion Polymerization Recipe<sup>22</sup> Using a Thermal Initiator at 70°C

	Ingredient	Weight (g)	Comment
Monomer	<i>N</i> -isopropylacrylamide (NIPAM)	7.0	1.4% solids content
Crosslinker	Methylenebis(acrylamide) (MbAA)	0.7	10% based on monomer
Surfactant	Sodium Dodecyl Sulfate (SDS)	0.094	0.65 mM based on the aqueous phase
Initiator	Potassium Persulfate (KPS)	0.28	2.07 mM based on the aqueous phase
Medium	Deionized water (H <sub>2</sub> O)	500.0	–

these particles essentially act as nanowater reservoirs. If these nanowater reservoirs are encapsulated by another rigid polymer, these core-shell particles could potentially be useful as microreactors for water phase reactions, which can be triggered by temperature, as a thermosensitive drug carrier by incorporating biocompatible shell polymer, as a nanosponge to absorb or release moisture to slow down corrosion in some coatings applications, and as hollow microspheres by using water as the blowing agent. The synthesis of these particles may open an interesting novel field of nanowater encapsulation and its applications. For comparison purposes, the PNIPAM encapsulation was carried out both below and above the VPTT via semibatch or seeded semibatch polymerization processes.

## EXPERIMENTAL

### Materials

*N*-isopropylacrylamide (NIPAM; 99%, VWR International, Bridgeport, NJ) was recrystallized from mixtures of toluene and hexane (in a volume ratio of 2 : 3). *N,N'*-methylenebisacrylamide (MbAA; 99%, Fisher Scientific, Pittsburg, PA), potassium persulfate (KPS; Fisher Scientific), *L*-ascorbic Acid (99%, Sigma-Aldrich, St. Louis, MO), hydrogen peroxide, (H<sub>2</sub>O<sub>2</sub>; 35%, Sigma-Aldrich), ferrous sulfate (FeSO<sub>4</sub>·7H<sub>2</sub>O; Fisher Scientific), and sodium dodecyl sulfate (SDS; Sigma-Aldrich) were all used as received.

### Synthesis of poly(*N*-isopropylacrylamide) using a thermal initiator

The preparation of PNIPAM seed particles using a thermal initiator was carried out according to Pelton's recipe<sup>22</sup> shown in Table I. The NIPAM, MbAA, SDS, and 470 g deionized water were added to a 500-mL three-neck reactor fitted with a reflux condenser, a glass stirring rod with a Teflon half-moon impeller, and a nitrogen bubbling tube. The reactor was kept immersed in a thermostated water bath maintained at 70°C. The solution was stirred at 200 rpm for 30 min with nitrogen purging. Potassium persulfate was dissolved in 30 g of deionized water and injected into the reactor to initiate the reaction. Polymerization was carried out at 70°C for 4 h.

### Determination of conversion

High-performance liquid chromatography [HPLC; Supelco (Belefonte, PA), with an LC-CN column and a UV-Vis detector (Beckman Instruments, Fullerton, CA)] was used to measure the conversion of NIPAM monomer because NIPAM is a solid at room temperature (melting point = 65°C) and conventional gravimetric analysis cannot be used to evaluate the polymerization conversion with a solid monomer. Deionized (DI) water was used as the mobile phase with a flow rate of 0.70 mL/min. The samples were centrifuged for 3 h at 9000 rpm to separate any particles that could clog the HPLC column before injection into the HPLC.

### Determination of particle size

The particle diameter and size distributions of the latex particles were measured by dynamic light scattering (Nicomp, Model 370, Santa Barbara, CA) at 25°C and by capillary hydrodynamic fractionation at 35°C (CHDF 1100 and 2000, Matec Applied Sciences, Northborough, MA). They were also measured (in a dry state) by transmission electron microscopy (TEM, Philips 400T, Eindhoven, Netherlands), measuring 600 particles for each sample.

Dynamic light scattering (DLS) analysis as a function of temperature was also carried out using a Brookhaven Instruments (Hulstville, NY) commercial laser light scattering spectrometer. The spectrometer has two lasers [JDS Uniphase 50 mW diode-pumped solid-state (DPSS) laser (model  $\mu$ Green-SLM) operating at 532 nm (Huntington Valley, PA) and a Melles Griot 35 mW He-Ne laser (model 05-LHP-928) (Albuquerque, NM)] operating at 633 nm and a Brookhaven Instruments (BI 9000AT) correlator. The measurements were carried out using the JDS laser. The sample chamber was thermostated during the measurement. The intensity-intensity time correlation functions were analyzed by the CONTIN method.

Transmission electron microscopy shadowing experiments were carried out according to the following procedure. A drop of highly diluted latex sample was first dried on a TEM grid. This sample was then coated by gold vapor deposition. By tilting the gold vapor source to a certain degree to the sample, a particle "shadow" was created, representing

**TABLE II**  
**Recipe Used for Multistage Polymerization with Styrene as the Second Monomer at 70°C**

Ingredient		Weight (g)	Comments
Monomer	NIPAM	1.4	1.4% solids content
Crosslinker	MBMA	0.14	10 wt % based on monomer
Surfactant	SDBS	0.0188	0.65 mM
Initiator	KPS	0.056	2.07 mM
Medium	H <sub>2</sub> O	100	–
Second Monomer	Styrene	6.55	–
Second Surfactant	SDBS	0.544	Dissolved in 7.2 g DI water
Feed Rate (μL/min)		30 (start feeding at 15 min of reaction)	
Reaction Time (hr)		5.25 h	

an area not coated by gold. This tilting angle was determined by using standard polystyrene particles as an internal standard.

#### Determination of linear polymer fraction in PNIPAM

Ultracentrifugation was used to separate the linear PNIPAM fraction from the crosslinked PNIPAM fraction. The samples were ultracentrifuged at 30 K rpm at 5°C for 2 h. The soluble linear PNIPAM was present in the top layer of the centrifuge tube, whereas the crosslinked PNIPAM with a small amount of water was present at the bottom of the tube. By drying the samples obtained from the top layer and the bottom layer of the centrifuge tube, the solids contents of the two layers could be obtained through gravimetric analysis. As the original PNIPAM latex solids content is known, the linear fraction of PNIPAM can be calculated.

#### Sucrose density gradient experiment

To determine the density of the second-stage latex polymer particles, a sucrose density gradient experiment was carried out. A series of aqueous sucrose solutions were prepared with different concentrations (3, 10, 17, 24, 34, and 44%) to obtain different densities (1.01, 1.04, 1.07, 1.10, 1.15, and 1.21 g/cm<sup>3</sup>). One milliliter each of the sucrose solutions were sequentially layered in a test tube in order of decreasing density. One milliliter of the latex was then layered on top of the sucrose density gradient column. The samples were then ultracentrifuged at 30 K rpm at 5°C for 1 h. Depending on the position of the latex in the tube after centrifugation, the density of the latex was determined.

#### Cleaning of latex

The latex was cleaned by a serum replacement process.<sup>23</sup> After diluting the latex to 5% solids content in water, the latex was charged into a serum replace-

ment cell, which was fitted with a 200 nm pore size membrane. The latex was cleaned by passing 30 to 40 residence volumes (400 mL) of DI water through the latex. The serum replacement process was continued until the conductivity of serum was close to that of deionized water (0.35 μΩ cm<sup>-1</sup>).

#### Shell synthesis by semibatch polymerization process at 70°C

The method employed to prepare a core-shell structure was a semibatch process with *in situ* generation of the seed latex. The detailed recipe is shown in Table II. A 200 mL four-neck flask was fitted with a reflux condenser, a glass stirring rod with a Teflon half-moon impeller, and a rubber stopper with two tubes for feeding St and SDBS aqueous solution and a nitrogen bubbling tube. After the first stage PNIPAM synthesis was carried out for 15 min (the conversion reached 85%, thus forming an *in situ* seed), styrene and SDBS (which was dissolved in 7.2 g water), were fed into the reactor at a rate of 30 μL/min (in some cases a feed rate of 15 or 60 μL/min was used). No further initiator was added. The reaction was carried out at 70°C for 5 h.

#### Shell synthesis by a seeded semibatch process at 28°C

The preparation of poly(*N*-isopropylacrylamide) seed particles with a compatibilizing polystyrene tie layer was carried out in the same reactor setup as described previously for preparing the poly(*N*-isopropylacrylamide) seed particles (at 70°C), and the recipe used is the same as that shown in Table I. After the polymerization was carried out for 15 min (85–90% conversion), 1 g of styrene was added in one shot into the reactor. The reaction was carried out for another 3 h and 45 min to reach full conversion.

A semibatch emulsion polymerization process was then employed to synthesize a styrene shell layer around the PNIPAM seed particles (synthesis described earlier). The recipe used is shown in Table

**TABLE III**  
**Recipe Used for the Second-Stage Seeded Semibatch Emulsion Polymerization of Styrene Around PNIPAM Seed Latex at 28°C**

Ingredient		Weight (g)	Comment
Seed	PNIPAM latex with PS Tie layer	100	1.5 % solids content
Shell Monomer	St	9.1	–
Surfactant	SDBS	0.946	Dissolved in 10 g DI water
	35% H <sub>2</sub> O <sub>2</sub>	0.0657	0.23%, based on monomer
Initiator	AA	0.0130	0.13%, based on monomer
	FeSO <sub>4</sub> ·7H <sub>2</sub> O	0.0014	Fe (II) 37 ppm
Buffer	NaHCO <sub>3</sub>	0.0050	–
2nd Stage Feed	SDBS	30	–
Rate (μL/min)	St	30	–

III. The PNIPAM seed latex (that employed the compatibilizing styrene tie layer) was charged into the same 200-mL four-neck reactor setup as used previously. A redox initiator pair, hydrogen peroxide, and ascorbic acid with a trace amount of iron were used for this reaction. All of the hydrogen peroxide and iron and half of the ascorbic acid were injected at the beginning of the polymerization. The remaining portion of ascorbic acid was mixed into an aqueous surfactant solution and fed into the reactor to start the polymerization. St and SDBS were fed into the reactor separately at a rate of 30 μL/min, and the polymerization was carried out at 28°C for 6 h (below 34°C, the VPTT of the PNIPAM seed) with stirring at 200 rpm. After finishing the feed stage, the reaction was continued for one more hour.

## RESULTS AND DISCUSSION

### N-isopropylacrylamide polymerization

N-isopropylacrylamide polymerization was based on the surfactant-free recipe developed by Pelton and coworkers.<sup>22</sup> In this polymerization, the surfactant concentration was 0.65 mM based on the aqueous phase, which was much lower than 11.0 mM, its critical micelle concentration (CMC).<sup>24</sup> Therefore, the particles obtained resulted from heterogeneous nucleation instead of micellar nucleation.<sup>25</sup> HPLC results indicated that the conversion was quite close to 100% and there was no measurable amount of monomers that remained.

Because of the large difference in hydrophobicities between PS and PNIPAM, a monomer addition strategy was employed. If the second-stage styrene monomer could polymerize and form a thin layer in the outer edge of the seed particles, this would improve the compatibility between the PNIPAM core and PS shell polymers. For this to occur, the feeding of the second stage monomer was started when the monomer conversion of the first stage of the polymerization reached 85–90%. To determine

when to start feeding of the shell monomer, the kinetics of PNIPAM polymerization was studied by using a Mettler RC-1 calorimetric reactor at 70°C. Analysis of the kinetics showed that the conversion reached 80–90% during the first 12 to 20 min of the reaction. The particle size was ~ 290 nm as measured by DLS after 15 min of reaction. The polymerization rate reached a maximum after 4.5 min of the reaction. The results agreed with Pelton's observation that PNIPAM polymerization was a very fast reaction.<sup>25</sup>

By using dynamic light scattering, the particle size and size distributions of PNIPAM particles were measured. The PNIPAM particles exhibited narrow size distributions with particle diameters ~ 300 nm at room temperature, as shown in Table IV. The PNIPAM particle diameters measured by dynamic light scattering (DLS) were quite different from the sizes measured by CHDF at 35°C due to the temperature difference between the two measurements, the former being below the VPTT and the latter above the VPTT. The dry particle size was 128 nm measured by TEM and is shown in Table IV and Figure 1. It was reported that PNIPAM particles are oblate-disk-shape when imaged by SEM<sup>26</sup> resulting from the deformation of PNIPAM during sample preparation. Therefore, the dry particle size obtained from TEM might be larger than its true particle size.

It was hypothesized that during the seed stage, there is also linear PNIPAM formed. Ultracentrifugation was used to separate the linear PNIPAM from crosslinked PNIPAM particles. Using a typical recipe, 11% linear PNIPAM polymer was found in the PNIPAM latex. Pelton and coworkers<sup>25</sup> showed that

**TABLE IV**  
**PNIPAM Seed Particle Size Analysis**

Measurement methods	$D_n$ (nm)	$D_w$ (nm)	$D_l$ (nm)	PDI
DLS (RT)	306	–	308.8	1.01
CHDF (35°C)	149	151	–	1.03
TEM (dry state)	128	136	–	1.06

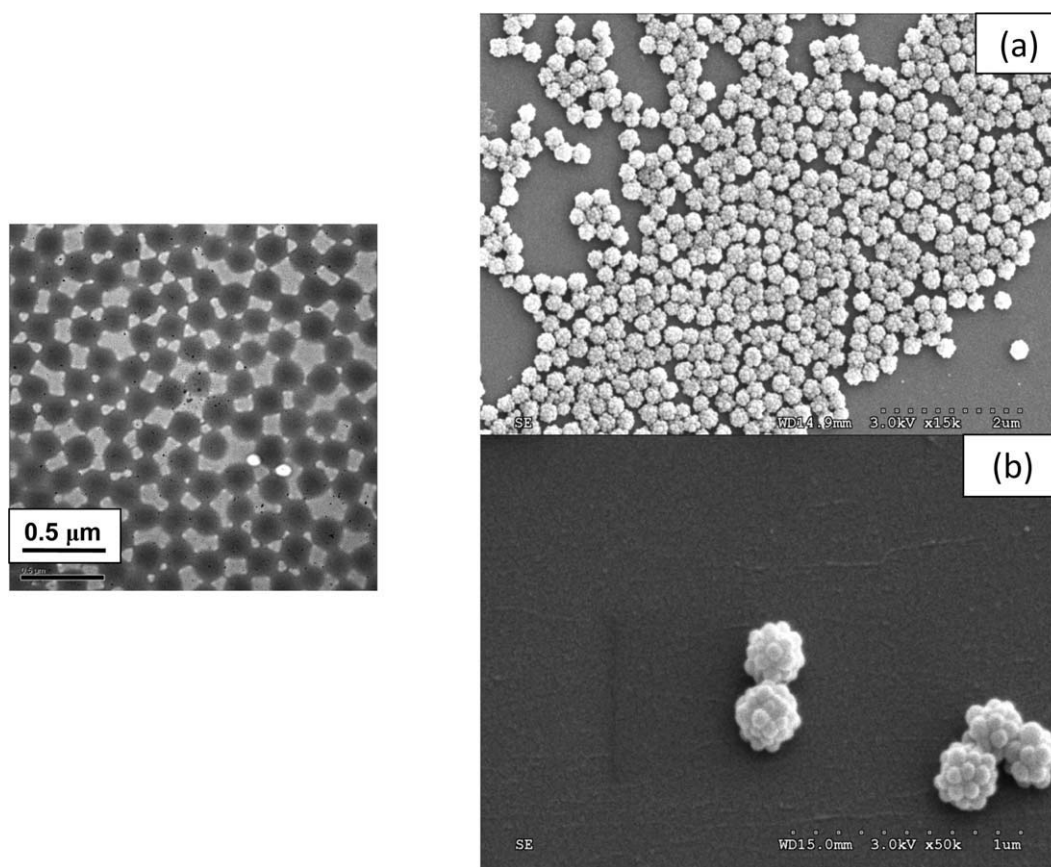


**Figure 1** (Left) TEM micrographs of PNIPAM particles; (Right) synthesized by a semibatch polymerization method; (Right) SEM micrographs of PNIPAM/PS particles synthesized by a semibatch polymerization method. (a) 15 K, and (b) sample stage tilted  $20^\circ$ ,  $\times 50$  K.

the MbAA crosslinker was consumed more quickly than was the NIPAM. Therefore, it would be reasonable to expect that there is a MbAA concentration gradient within the PNIPAM particles, i.e., a high concentration in the center of the particles and a low concentration on the particle surface.

### Shell formation stage

The semibatch polymerization was a process consisting of the *in situ* generation of seed latex followed by styrene monomer feed addition at 15 min into the polymerization (85 to 90% NIPAM conversion). The feed consisted of styrene as well as surfactant (SDBS) and were slowly fed to the reactor. This process is designed to synthesize the PNIPAM/PS core/shell particles at a temperature higher ( $70^\circ\text{C}$ )

than the LCST. Styrene was added before the NIPAM polymerization was complete to slowly change the composition of the polymer layer between the core and the shell.

The resulting structured particles were characterized by DLS, CHDF, and TEM. The results are shown in Table V. The particle size obtained at the end of reaction was about 300 nm as measured by DLS at room temperature. Two populations of particles appeared in the CHDF analysis, i.e., 40 nm and 260 nm particles (CHDF measurements were carried out at  $35^\circ\text{C}$ , just above the PNIPAM's volume phase transition temperature (VPTT)). Although the population of small particles was 91.6% by number, they were only 4.5% by weight. The particle size measured by TEM was 250 nm by weight. Only a few small polystyrene particles were

**TABLE V**  
Particle Size Analysis by DLS, CHDF, and TEM for PNIPAM/PS Particles Prepared by Semibatch Polymerization

Diameter	DLS	CHDF	TEM	TEM bumps
$D_n$ (nm)	293	36 (91.6%)	246	59
$D_l$ (nm)	310	—	—	—
$D_w$ (nm)	—	47 (4.5%)	250	64

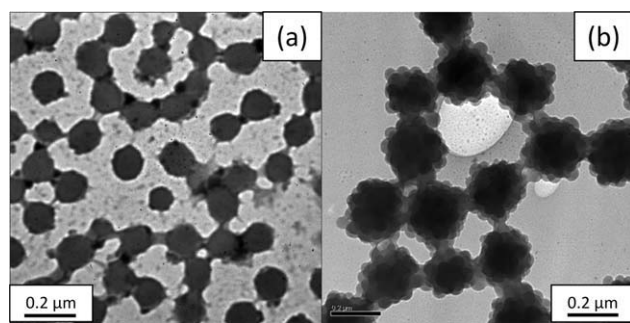


**Figure 2** TEM micrographs of: (a) PNIPAM seed particles polymerized with a styrene compatibilizing tie layer and (b) second stage particles prepared by seeded semibatch polymerization.

observed by TEM. The large particle size measured by CHDF agrees with the TEM measurement and also was close to the DLS result. The SEM micrographs given in Figure 1 (right; a, b) showed a uniform “raspberry” structure. The size of small domains was in the range of 50–60 nm, which was too small to be PNIPAM particles. In addition, no individual PNIPAM particles were observed in the TEM or SEM. Therefore, it is most likely that these small domains were PS. It appears that small PS particles were generated in the aqueous phase first and then heteroflocculated with the PNIPAM particles. This correlates with the size of small particles detected by CHDF particle measurements.

In the seeded semibatch process, a core polymer was first synthesized by batch polymerization (with a styrene tie layer incorporated) in a first stage process at 70°C. Styrene monomer then was slowly fed to the latex seed obtained from the first stage of the polymerization and polymerized by a semibatch polymerization process. Both the seed particles and particles obtained by the seeded semibatch reaction were characterized by dynamic light scattering, CHDF, and TEM (Fig. 2). The results are shown in Table VI. The particle size of the PNIPAM seed particles with a tie layer present, measured by dynamic light scattering, was  $\sim 300$  nm at room temperature, which is close to the normal PNIPM particle size. The particle size of the PNIPAM with a tie layer, measured by CHDF, was 160 nm

(weight-average diameter,  $D_w$ ), which was 10 nm larger than the PNIPAM particle size measured by CHDF at 35°C. One possible explanation for this difference is that in the presence of the tie layer, the PNIPAM particles are a bit more rigid, and hence, release less water than the normal PNIPAM particles at a higher temperature than the VPST of PNIPAM.

The diameter of the PNIPAM particles with a tie layer present was measured by TEM to be  $\sim 148$  nm ( $D_w$ ), which again is close to the normal PNIPAM particles without a tie layer present. For the final latex particles obtained from the seeded semibatch reaction, the particle diameter obtained by dynamic light scattering was  $\sim 300$  nm (intensity-average diameter;  $D_I$ ), CHDF measurements showed that there were two crops of particles, 50 nm small polystyrene particles and 290 nm large particles ( $D_w$ ). As was shown in the semibatch process, small polystyrene particles existed, but they were only present at a concentration of 6.3% by weight. From TEM analysis, the particle size of the final latex was  $\sim 260$  nm ( $D_w$ ). When comparing the CHDF results with TEM results, there is good agreement. It is the first time that the large particle size observed in the CHDF was nearly equal to the large particle size measured by TEM which may imply that there may be a PS layer around PNIPAM seed particle to prevent the particles from further shrinkage during the drying process. The small particles observed in the CHDF measurements could be small polystyrene particles generated in the second stage.

Figure 2 shows the morphology of the PNIPAM particles with a tie layer present and the resulting final particles obtained from the seeded semibatch process. It can be clearly seen that the seed particles increased in size from 150 to 260 nm ( $D_w$ ) as measured by TEM. In addition, the same uniform “raspberry” structure was observed. There were not many individual PNIPAM particles observed by TEM. This may indicate that although these two reactions were carried out at different conditions, the “raspberry” structure may be a result of the same mechanism.

In both cases, the domains observed on the final particles were smooth hemispheres ( $\sim 50$ –60 nm),

**TABLE VI**  
Particle Size Analysis by DLS, CHDF, and TEM for PNIPAM Particles Prepared with a Tie Layer Present and the Particles Obtained from a Seeded Semibatch Reaction

	Diameter	DLS	CHDF	TEM
PNIPAM seed particles with tie layer	$D_n$ (nm)	297	157	144
	$D_I$ (nm)	310	–	–
	$D_w$ (nm)	–	160	148
	PDI	1.05	1.02	1.04
Particles from seeded-semibatch polymerization	$D_n$ (nm)	292	44 (94.8%)	301 (5.0%)
	$D_I$ (nm)	301	–	–
	$D_w$ (nm)	–	55 (6.3%)	305 (91.7%)

and they were too small to be PNIPAM particles. Therefore, these domains were probably PS. Some other reports also showed that copolymerizing NIPAM with styrene<sup>27</sup> or with acrylonitrile sometimes also resulted in a “raspberry” structure, but not a smooth hemisphere structure as shown in our study. It is believed that those “raspberry” structures resulted from phase separation while the polymerizations were carried out in the emulsifier-free system. However, in this research, a certain amount of surfactant was used in the second stage. Small PS particles may be generated in the aqueous phase first and then most likely heteroflocculate with the PNIPAM particles, generating the “raspberry” structured particles. The mechanism study on this multi-stage method will be discussed in a subsequent paper.

To correlate the expected core and shell particle size, we need to know the exact size of the core particles. By using a conventional method such as TEM, we determined that the dry particle diameter was  $\sim 140$  nm. However, according to Crowther and Vincent,<sup>26</sup> deformation of PNIPAM particles occurs during TEM or SEM sample preparation and oblate-disk-shape or ellipsoids were observed under SEM analysis.

A static light scattering (SLS) method was utilized to determine the dry particle size. Generally speaking, SLS is applied to determine the weight-average molecular weight ( $M_w$ ) for molecules in solution. However, in this case, each particle, instead of each molecule, is regarded as a separate unit. Therefore, the weight-average molecular weight that is obtained in these measurements represents the particle molar weight. A standard Zimm plot of the SLS data for PNIPAM particles is shown in Figure 3. When the theta angle was extrapolated to zero (the theta angle is the angle between the incident light and scattered light), the intercept is the inverse of the molar weight. When the concentration was extrapolated to zero, the intercept is also the reciprocal of molar weight of the particle. It is also possible to obtain the radius of gyration ( $R_g$ ) from the slope of the  $c = 0$  line. The molar weight of the particle was  $7.00 \times 10^8$  g/mol when theta was extrapolated to zero, whereas the molar weight of the particles was  $6.75 \times 10^8$  g/mol when the concentration was extrapolated to zero. There is good agreement between the two molecular weights. As the density of PNIPAM is known<sup>17</sup> to be  $1.269$  g/cm<sup>3</sup>, the dry particle size of PNIPAM was calculated to be about 120 nm in diameter. Then, the particle number obtained was  $1.34 \times 10^{16}$ /L by dividing the mass of NIPAM by the mass of one particle.

The calculated radius of gyration was 131 nm. The  $R_g/R_h$  value was 0.87 at room temperature, which is close to the reported value in the literature, 0.85.<sup>28</sup> A

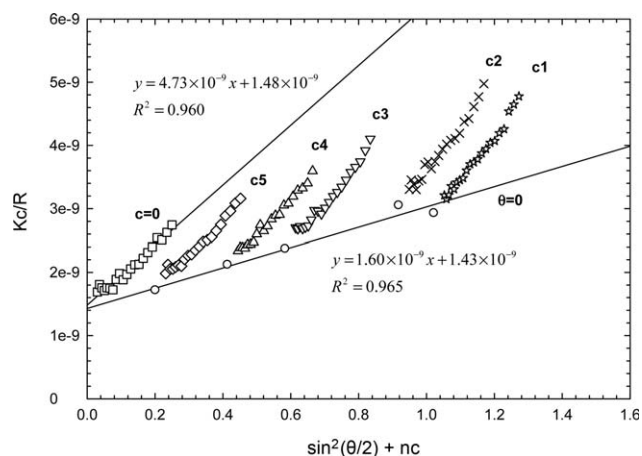


**Figure 3** Zimm plot of PNIPAM dispersion obtained from SLS. The concentrations used were:  $c_1: 2.04 \times 10^{-4}$  g/cm<sup>3</sup>,  $c_2: 1.83 \times 10^{-4}$  g/cm<sup>3</sup>,  $c_3: 1.17 \times 10^{-4}$  g/cm<sup>3</sup>,  $c_4: 8.29 \times 10^{-5}$  g/cm<sup>3</sup>, and  $c_5: 4.04 \times 10^{-5}$  g/cm<sup>3</sup>.

ratio of 0.775 usually indicates a uniform internal structure.

As it was not known how precise the SLS method was in determining the PNIPAM dry particle size, another TEM technique, namely a shadowing technique, was employed for determining the PNIPAM dry particle size. Under TEM, it is possible to observe the “shadow” of the particles. The greater the particle height, the longer the shadow will be. Monodisperse polystyrene (PS) particles were used as a standard to determine the tilt angle, assuming that monodisperse PS particles do not exhibit any deformation during the shadowing process. As the length of the shadow and the particle diameter can be measured, the tilt angle can be calculated, which was  $28.5^\circ$ . The  $D_z$  of PNIPAM can be calculated based on the known tilt angle and the measured PNIPAM shadow length. Figure 4 shows TEM micrographs of the PS monodisperse particles and PNIPAM particle in the shadowing experiment. The PNIPAM particles dimensions are shown in Table VII. Assuming that the PNIPAM particles are ellipsoidal in shape, by using the total volume of one PNIPAM particle, its particle diameter was back-calculated to be 132 nm. (The calculator was obtained from <http://www.csgnetwork.com/volumeellipsoid.html>). Comparing this result to the particle diameter obtained from SLS, the particle size obtained from the shadowing experiment is 12 nm larger, which may be because there was a gold coating layer present (needed for the SEM sample preparation). Therefore, these two experiments agree with each other reasonably well. It is reasonable to conclude that the dry particle size of PNIPAM was 120 nm.

Based on the obtained PNIPAM particle size and the known amount of styrene fed, the final

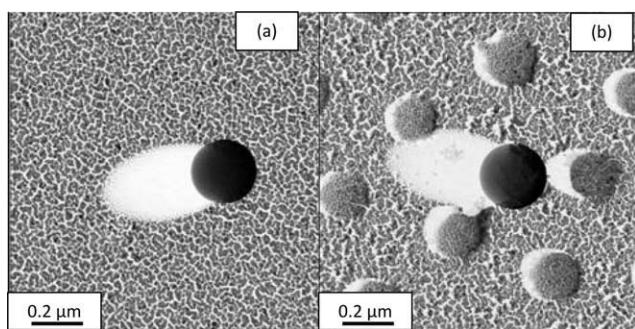


**Figure 4** TEM micrographs of: (a) monodisperse polystyrene particles, and (b) monodisperse polystyrene particles mixed with PNIPAM particles in shadowing experiments with a gold coating.

calculated core/shell size was 220 nm, which was 20–30 nm smaller than the core/shell particle size determined by TEM. This may imply that there is some water retained within the particles.

It is well known that PNIPAM is sensitive to temperature. By using DSC, it was determined that the transition temperature of the synthesized PNIPAM was 34.9°C. The same PNIPAM particles were tested by dynamic light scattering. The results are shown in Figure 5. When the testing temperature was 20°C, the particle size was 270 nm. There was a slight reduction in particle size when the temperature was changed from 20 to 28°C. This result agreed with what Pelton observed in his study.<sup>29</sup> The significant change in particle size occurred when the temperature was changed from 28 to 35°C, which indicated that the PNIPAM transition occurred. After the temperature was increased higher than 35°C, the particle radius remained at around 70 nm. Monodisperse polystyrene particles were used as a control since their particle size should remain constant as the temperature was increased from 20 to 40°C. From Figure 5, it is shown that the diameter of the monodisperse polystyrene particles was 280 nm with some fluctuation as the temperature varied. This may occur in this experiment since the actual sample temperature cannot be directly detected. Therefore, there was some error between the actual temperature and the displayed temperature, which may affect the viscosity value used in the size calculation. It was found that the PNIPAM/PS core/shell particles exhibited a stable size at 270 nm (135 nm in radius) while

**TABLE VII**  
Results of PNIPAM Dimensions Obtained from TEM Shadowing Experiments

$R_x$ (nm)	84.0
$R_y$ (nm)	84.0
$\Theta$ (°)	28.5
$R_z$ (nm)	41.1
$V$ (nm <sup>3</sup> )	1.2E + 06

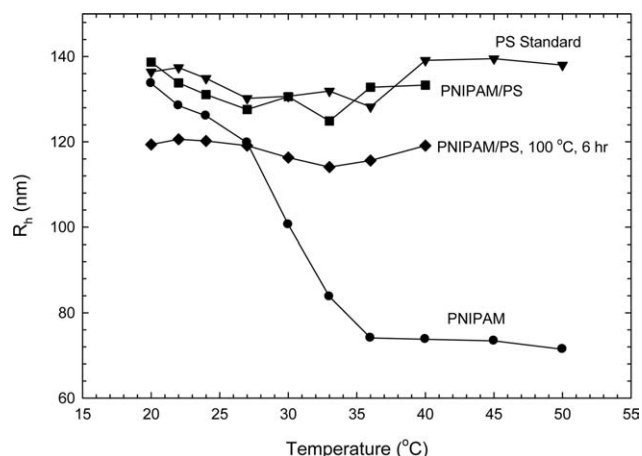
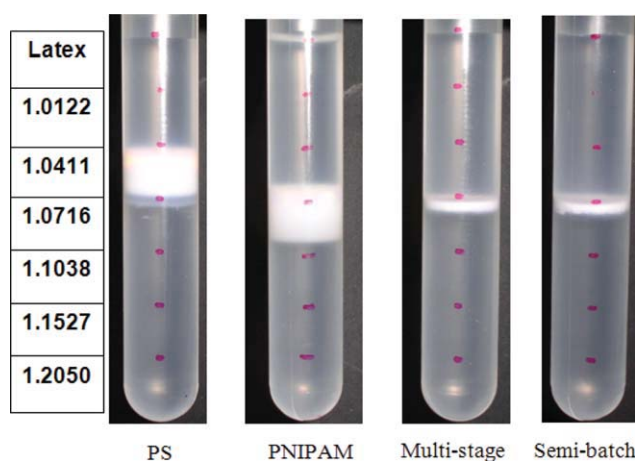


**Figure 5** Temperature dependence of the hydrodynamic radius ( $R_h$ ) measured by DLS.

changing the temperature. After heating at 100°C for 6 h, the core/shell particle size remained  $\sim$  240 nm in diameter. The particle size of PNIPAM/PS obtained from DLS agreed with the previous TEM results. In both cases, the size did not change as the temperature was varied from 20 to 40°C, which may indicate good encapsulation of PNIPAM by polystyrene.

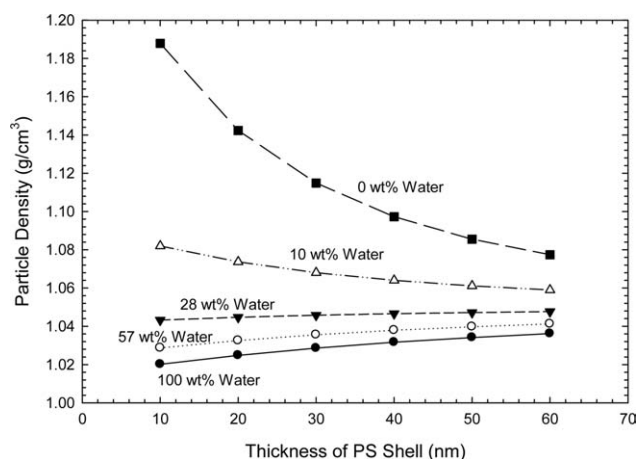
Another approach, using a density gradient experiment, was employed to test whether the PS grew around the PNIPAM seed particles to form a shell or was formed inside the PNIPAM particles. Density gradient experiments were carried out based on the idea that the particles with a PNIPAM core and a PS shell present containing water inside the PNIPAM core would have a lower density than PNIPAM/PS copolymer particles, which would have almost no water retained. The densities of the particles were measured by using a density gradient column and compared with the densities obtained by theoretical calculations.

Figure 6 shows the density gradient results. The density of PNIPAM was between 1.04 and 1.07 g/cm<sup>3</sup>, which is smaller than the reference PNIPAM density, 1.269 g/cm<sup>3</sup>. The reason could be that the PNIPAM particles had released some water into the column during the centrifugation, but there was still some water remaining inside the particles. The density of PS was about 1.04 g/cm<sup>3</sup>, which agreed with the reference density, 1.05 g/cm<sup>3</sup> at 20°C.<sup>30</sup> A series of theoretical densities were calculated based on a PNIPAM/PS core-shell structure and are shown in Figure 7. In the theoretical density calculations, 1.269 g/cm<sup>3</sup> was assumed as the density of PNIPAM and 1.05 g/cm<sup>3</sup> was assumed as the density of PS. The densities of particles with 120 nm cores, different diameter shells, and different amounts of encapsulated water were calculated. The density gradient experiment indicated that the densities of the



**Figure 6** Density Gradient results. Image of density gradient column after centrifugation at 30 K rpm for 1 h at 5°C. Density values ( $\text{g}/\text{cm}^3$ ) in column were indicated at left. [Color figure can be viewed in the online issue, which is available at [www.interscience.wiley.com](http://www.interscience.wiley.com).]

particles obtained by using both synthesis methods were in the range of 1.04–1.07  $\text{g}/\text{cm}^3$ . From Figure 7, the calculated core/shell particle with a 120 nm dry core with no water encapsulated would have a density between 1.09 to 1.19  $\text{g}/\text{cm}^3$ , which was higher than the particle density that was obtained from the density gradient experiment. This implies that some water may be retained within the particles. This result also agrees with the theoretical calculation based on PNIPAM dry particle size measured by SLS. Figure 7 shows that with 10 wt % water retained a density between 1.08 to 1.05  $\text{g}/\text{cm}^3$  should be obtained, and with 28 wt % water, the density should be between 1.04–1.05  $\text{g}/\text{cm}^3$ . As the density did not change significantly in this range, we are not able to identify the exact amount of water retained by density measurements. However, the calculation did show that the obtained core/shell particles may have 10–30% water retained. This find-



**Figure 7** Theoretical calculations of PNIPAM/PS core/shell particle densities (120 nm PNIPAM core).

ing agrees with what Pelton reported, that even though the temperature is higher than its VPTT, PNIPAM particles can still retain  $\sim 30\%$  water.<sup>28</sup>

## CONCLUSIONS

Crosslinked PNIPAM particles were synthesized by precipitation polymerization. The conversion was close to 100% as determined by HPLC. The particle diameter in water determined by DLS was  $\sim 300$  nm at room temperature and the size distribution was narrow. The dry particle diameter was  $\sim 140$  nm, as determined by TEM, which may be slightly larger than the actual particle size due to deformation during TEM sample preparation.

The resulting crosslinked PNIPAM particles have a VPTT at 34.9°C and a  $T_g$  at 154°C. The linear fraction of PNIPAM was separated and measured to be  $\sim 11\%$  for the typical recipe. The PNIPAM polymerization conversion-time profile was studied in a Mettler RC-1 reaction calorimeter. The conversion reached 85% in the first 15 min of the reaction.

Two different methods were developed to produce PNIPAM/PS hydrophilic core/hydrophobic shell particles, i.e., semibatch or seeded-semibatch polymerization. In both methods, uniform “raspberry” structures were obtained in which polystyrene formed small domains on the PNIPAM particles. The resulting PNIPAM/PS particle size was 300 nm as determined by DLS. The dry particle size was in the 250–260 nm range and the PS domain size was  $\sim 50$ –60 nm, measured by TEM. The reason for the “raspberry” structure formation is probably by a heteroflocculation mechanism to be discussed in a subsequent paper.

The dry PNIPAM particle size was analyzed by static light scattering methods (SLS) and a TEM shadowing technique. The results indicated that the dry PNIPAM particle size was  $\sim 120$  nm. The PNIPAM/PS core/shell particles have been studied by dynamic light scattering (DLS) and results show that the particle diameter did not change when temperature was increased over the range from 20 to 40°C. This indicates that PNIPAM was fully encapsulated by PS. A density gradient experiment showed that the obtained “raspberry” structured PNIPAM/PS particle has a density in the range of 1.04–1.07  $\text{g}/\text{cm}^3$ . By comparing this density with a theoretical calculation, our calculation indicates that  $\sim 10$ –30% water may be retained within the PNIPAM/PS particles.

## References

1. Taniguchi, T.; Duracher, D.; Delair, T.; Elaissari, A.; Pichot, C. *Colloids Surf B Biointerfaces* 2003, 29, 53.
2. Elaissari, A. *Handbook of Surface and Colloid Chemistry*, 3rd ed.; CRC Press: Boca Raton, FL, 2009; p 539.

3. Duracher, D.; Sauzedde, F.; Elaïssari, A.; Perrin, A.; Pichot, C. *Colloid Polym Sci* 1998, 276, 219.
4. Ramanan, R. M. K.; Chellamuthu, P.; Tang, L. P.; Nguyen, K. T. *Biotechnol Prog* 2006, 22, 118.
5. Chen, C. W.; Chen, M. Q.; Serizawa, T.; Akashi, M. *Chem Commun* 1998, 831.
6. Tkuyama, H.; Yanagawa, K.; Sakohara, S. *Separ Purif Technol* 2006, 50, 8.
7. Sun, Q.; Deng, Y. *Langmuir* 2005, 21, 5812.
8. Andersson, M.; Hietala, S.; Tenhu, H.; Maunu, S. L. *Colloid Polym Sci* 2006, 284, 1255.
9. Zhu, D.; Weng, F.; Gao, C.; Xu, Z. *Front Chem Eng China* 2008, 2, 253.
10. Zhang, F.; Wang, C.-C. *Colloid Polym Sci* 2008, 286, 889.
11. Weda, P.; Trzebicka, B.; Dworak, A.; Tsvetanov, C. B. *Polymer* 2008, 49, 1467.
12. Peng, M.; Wang, H.; Chen, Y. *Mater Lett* 2008, 62, 1535.
13. Musch, J.; Schneider, S.; Lindner, P.; Richtering, W. *J Phys Chem B* 2008, 112, 6309.
14. Wu, J.; Zhuo, B.; Hu, Z. *Phys Rev Lett* 2003, 90, 048304.
15. Keerl, M.; Pedersen, J. S.; Richtering, W. *JACS* 2009, 131, 3093.
16. Pelton, R. H. *J Polym Sci Part A: Polym Chem* 1988, 26, 9.
17. Andersson, M.; Maunu, S. L. *J Polym Sci Part B: Polym Phys* 2006, 44, 3305.
18. Glinel, K.; Sukhorukov, G. B.; Moehwald, H.; Khrenov, V.; Tauer, K. *Macromol Chem Phys* 2003, 204, 1784.
19. Makino, K.; Yamamoto, S.; Fujimoto, K.; Kawaguchi, H.; Ohshima, H. *J Colloid Interface Sci* 1994, 166, 251.
20. Zhu, P. W.; Napper, D. H. *Colloids Surf A Physicochem Eng Asp* 1995, 98, 93.
21. Xiao, X.; Chu, L.; Chen, W.; Wang, S.; Xie, R. *Langmuir* 2004, 20, 5247.
22. McPhee, W.; Tam, K. C.; Pelton, R. *J Colloid Interface Sci* 1993, 156, 24.
23. Ahmed, S. M.; El-Aasser, M. S.; Pauli, G. H.; Poehlein, G. W.; Vanderhoff, J. W. *J Colloid Interface Sci* 1980, 73, 388.
24. Gerrens, H.; Hirsch, G. In *Polymer Handbook*, 2nd ed.; Brandrup, J., Immergut, E. H., Eds.; Wiley: New York, 1975; p II-483.
25. Wu, S.; Pelton, R.; Hamielec, A.; Woods, D.; McPhee, W. *Colloid Polym Sci* 1994, 272, 467.
26. Crowther, H.; Vincent, B. *Colloid Polym Sci* 1998, 276, 46.
27. Taniguchi, T.; Duracher, D.; Delair, T.; Elaïssari, A.; Pichot, C. *Colloids Surf B Biointerfaces* 2003, 29, 53.
28. Pelton, R. *Adv Colloid Interface Sci* 2000, 85, 1.
29. Pelton, R. H.; Pelton, H. M.; Morpesis, A.; Rowell, R. L. *Langmuir* 1989, 5, 816.
30. Lide, D. R. *Handbook of Chemistry and Physics*, 85th ed.; CRC Press/Taylor and Francis: Boca Raton, Florida, 2004–2005.